



**HAL**  
open science

## Volatile organic compounds absorption in a structured packing fed with waste oils: Experimental and modeling assessments

Margaux Lhuissier, Annabelle Couvert, Abdoulaye Kane, Abdeltif Amrane,  
Jean-Luc Audic, Pierre-Francois Biard

### ► To cite this version:

Margaux Lhuissier, Annabelle Couvert, Abdoulaye Kane, Abdeltif Amrane, Jean-Luc Audic, et al.. Volatile organic compounds absorption in a structured packing fed with waste oils: Experimental and modeling assessments. Chemical Engineering Science, 2021, 238, pp.116598. 10.1016/j.ces.2021.116598 . hal-03245164

**HAL Id: hal-03245164**

**<https://hal.science/hal-03245164>**

Submitted on 10 Jun 2021

**HAL** is a multi-disciplinary open access archive for the deposit and dissemination of scientific research documents, whether they are published or not. The documents may come from teaching and research institutions in France or abroad, or from public or private research centers.

L'archive ouverte pluridisciplinaire **HAL**, est destinée au dépôt et à la diffusion de documents scientifiques de niveau recherche, publiés ou non, émanant des établissements d'enseignement et de recherche français ou étrangers, des laboratoires publics ou privés.

# Volatile organic compounds absorption in a structured packing fed with waste oils: experimental and modeling assessments

Margaux Lhuissier<sup>a</sup>, Annabelle Couvert<sup>a</sup>, Abdoulaye Kane<sup>b</sup>, Abdeltif Amrane<sup>a</sup>, Jean-Luc Audic<sup>a</sup>, Pierre-François Biard<sup>a</sup>

<sup>a</sup>Univ Rennes, Ecole Nationale Supérieure de Chimie de Rennes, CNRS, ISCR - UMR 6226, F-35000 Rennes, France

<sup>b</sup>UniLaSalle-Ecole des Métiers de l'Environnement, Campus de Ker Lann, 35170 Rennes, France

## Abstract

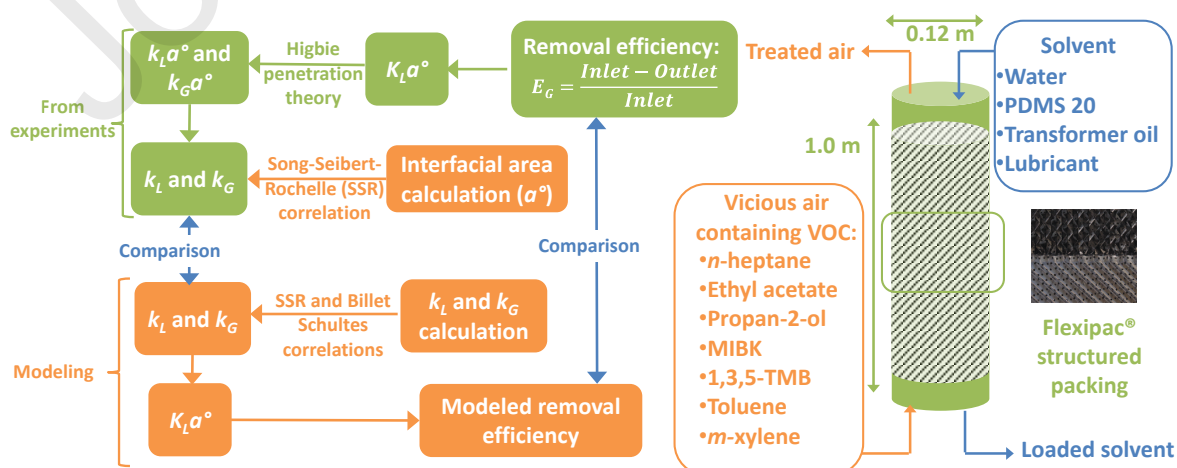
Volatile Organic Compounds (VOCs) having different polarities were absorbed in two viscous waste oils (a transformer oil and a lubricant, whose viscosities are equal to 19 mPa s and 79 mPa s, respectively) in a structured packing (1 m height) operated at counter-current. A synthetic hydrophobic solvent (PDMS 20, a silicone oil) and water were also used as reference solvents. Removal efficiencies of hydrophobic VOCs in silicone and transformer oils up to 80-90 % were measured. Nonetheless, owing to a higher viscosity, the removal efficiencies in the lubricant were significantly lower. A deconvolution procedure, based on the Higbie penetration theory, was developed to deduce the local mass transfer coefficients ( $k_L$  and  $k_G$ ) from  $K_L a^\circ$  values. These local coefficients were compared to the predictions of the models of Billet-Schultes (BS) and Song-Seibert-Rochelle (SSR), allowing to conclude that the SSR model better addresses the influence of the viscosity on  $K_L a^\circ$  than the BS model.

Corresponding author: [pierre-francois.biard@ensc-rennes.fr](mailto:pierre-francois.biard@ensc-rennes.fr), +33 2 23 23 81 49

## Keywords

Volatile organic compounds; waste oils; non-aqueous phase liquid; structured packing; absorption; mass transfer

## Graphical abstract



**Highlights**

- Absorption efficiencies of 7 VOCs were measured in a 1 m height structured packing
- Lubricant and transformer waste oils were investigated and compared to silicone oil
- Removal efficiencies up to 80-90% were measured for hydrophobic VOCs in transformer oil
- Overall mass transfer coefficients were deconvoluted to determine local coefficients
- The Song-Seibert-Rochelle models fairly predicted the influence of the viscosity on mass-transfer

Journal Pre-proofs

## 1. Introduction

Gas scrubbing, based on mass transfer from a gas phase to a liquid phase, can be applied to Volatile Organic Compounds (VOCs) treatment (Khan and Ghoshal, 2000; Ruddy and Carroll, 1993). Good removal efficiencies can be obtained using water as scrubbing liquid when the targeted VOCs are hydrophilic and/or acidic/basic (Biard and Couvert, 2013; Busca and Pistarino Chiara, 2003a, 2003b). Using water, packed columns operated at counter-current are selected most of the time at industrial scale, even if co-current intensified gas-liquid contactors, such as venturi scrubbers, aero-ejectors, static mixers, etc., could be advantageously used (Biard *et al.*, 2017). However, many alarming VOCs involved in different industrial sectors, such as BTEX (benzene, toluene, ethylene, xylene), alkanes, etc. are neutral and hydrophobic compounds. Therefore, replacement of water by an non-aqueous phase liquid (NAPL) to remove efficiently these compounds has been recently investigated (Bruneel *et al.*, 2018; Darracq *et al.*, 2012; Muñoz *et al.*, 2012, 2007). However, NAPL have typically viscosities from one to three orders of magnitude higher than water, making difficult to use co-current gas-liquid contactors and implying to select a counter-current packed column. Indeed, even if the higher viscosity of such solvents induces a higher mass transfer resistance in the liquid phase, liquids having viscosities up to two orders of magnitude higher than water can be successfully implemented in packed column according to several studies (Billet and Schultes, 1999, 1993a, 1991; Brunazzi *et al.*, 2002; Lhuissier *et al.*, 2020; Minne *et al.*, 2018; Song *et al.*, 2018, 2014).

Several authors studied at the laboratory scale different synthetic NAPLs for VOC absorption, especially silicone oils (Chiang *et al.*, 2012; Darracq *et al.*, 2010b, 2010a; Dumont *et al.*, 2012; Guillerm *et al.*, 2015; Patel *et al.*, 2016; Tatin *et al.*, 2015), phtalates such as di-2-ethylhexylphtalate (DEHP) (Bourgois *et al.*, 2008, 2006), adipates such as di-2-ethylhexyladipate (DEHA) (Hadjoudj *et al.*, 2004; Heymes *et al.*, 2006; Heymes *et al.*, 2006; Mhiri *et al.*, 2011; Monnier *et al.*, 2010; Monnier and Falk, 2011; Vuong *et al.*, 2009) or even ionic liquids (Camper *et al.*, 2006; Ferguson and Scovazzo, 2007; Guihéneuf *et al.*, 2014; Morgan *et al.*, 2005; Quijano *et al.*, 2011; Rodriguez Castillo *et al.*, 2019; Shiflett *et al.*, 2006; Shiflett and Yokozeki, 2006). To reduce the CAPEX related to synthetic NAPLs, cheaper waste oils such as mineral oils, composed of long chained alkanes (fresh and waste lubricant, biodiesel, cutting oil), have been also considered for VOC absorption (Bay *et al.*, 2006; Lalanne *et al.*, 2008; Ozturk and Yilmaz, 2006). Recently, Lhuissier *et al.* (Lhuissier *et al.*, 2018) measured the partition coefficients of several VOCs of different nature (either non-polar such as n-heptane or toluene, and polar such as propan-2-ol) in four waste oils (engine, hydraulic, transformer and vegetable oils). They demonstrated that the partition coefficients of these VOCs were lower than in silicone oils. These oils, due to their waste status, might contain volatile compounds and so could cause secondary emissions (Ozturk and Yilmaz,

2006). They showed that lubricant and transformer oils have low volatilities and are compatible with an absorption process.

Up to now, the assessment of NAPLs for VOCs absorption is mainly based on the determination of the partition coefficients of the VOC/NAPL system. Only two experimental studies assessed toluene mass transfer in DEHA and silicone oil in laboratory scale packed columns (Guillerm *et al.*, 2016; Frederic Heymes *et al.*, 2006), maybe because this kind of study is time-consuming and requires high footprint and expensive set-ups. These studies confirmed the potential of NAPL for VOC absorption but did not allow to determine the values of the local mass transfer coefficients ( $k_L$  and  $k_G$ ) and of the interfacial area ( $a^\circ$ ), which would allow to quantify accurately the influence of the solvents' characteristics (particularly the viscosity). In a previous paper, Lhuissier *et al.* (Lhuissier *et al.*, 2020) studied the hydrodynamics of lubricant and transformer waste oils in a lab-scale packed column of 0.12 m of internal diameter filled with a Flexipac® structured packing (packing height of 1 m). Their results showed that it was possible to operate counter-current packed column with viscous waste oils, especially the transformer oil. Lower loading and flooding gas superficial velocities than with water were however determined.

Nonetheless, no experimental study dealing with VOC absorption in waste oils in a packed column has been reported yet. Thus, the main purpose of this study was to assess the potential of lubricant and transformer oils for VOC absorption in the same packed column used by Lhuissier *et al.* (Lhuissier *et al.*, 2020), in comparison to water and a synthetic silicone oil. Seven VOCs of different natures and with various polarities (*n*-heptane, ethyl acetate, propan-2-ol, methylisobutylketone (MIBK), toluene, *m*-xylene and 1,3,5-trimethylbenzene (TMB), whose the octanol-water partition coefficients are summarized Table A.1 in Appendix) were selected (Lhuissier *et al.*, 2018). Both the VOC removal efficiencies and the overall volumetric liquid-phase mass transfer coefficients  $K_L a^\circ$  were determined. Then, a deconvolution procedure based on the Higbie penetration theory (Higbie, 1935) was applied to determine the local liquid and gas-side mass transfer coefficients ( $k_L$  and  $k_G$ ). Finally, the accuracy of the Billet-Schultes (BS) and Song-Seibert-Rochelle (SSR) models was evaluated. This procedure provided significant insights on the influence of the viscosity on the mass transfer rate.

## 2. Material and methods

### 2.1. Pilot-scale packed column

The experimental set-up, whose the main elements are the packed column operated at counter-current, a fan to feed the column with air at the bottom and a centrifugal pump to feed the fresh scrubbing liquid at the top of the column, has been already described by Lhuissier *et al.* (Lhuissier *et al.*, 2020). The packed column (internal column diameter  $D_{col} = 0.12$  m and height  $Z = 1$  m) was filled with a Flexipac® 500Z HC structured packing. The polluted air was generated through the vaporization of liquid VOC (contained in a gas-tight syringe) in the air stream by means of a syringe driver, to reach VOC concentrations between 20 and 110 mgC m<sup>-3</sup>. For each liquid absorbent, the gas and liquid superficial velocities were unvaried and selected in the loading zone (Lhuissier *et al.*, 2020), targeting values of the gas superficial velocities in the range 0.74-0.90 m s<sup>-1</sup> (Table 1). The VOC concentration at the inlet and the outlet of the column was quantified at steady-state by gas chromatography and flame ionization detection (GC Focus, oven temperature at 40°C, injector temperature at 125°C, detector temperature 190°C, carrier gas pressure at 2.5 kPa).

Table 1: Selected operating conditions

|   | Lubricant            | Transformer oil      | PDMS                 | Water                |
|---|----------------------|----------------------|----------------------|----------------------|
| Pressure $P$ (bar)                                    |                      | 1                    |                      |                      |
| Temperature $T$ (°C)                                  |                      | 25                   |                      |                      |
| Column diameter $D_{col}$ (m)                         |                      | 0.12                 |                      |                      |
| Packing height $Z$ (m)                                |                      | 1                    |                      |                      |
| Gas flow rate $F_G$ (m <sup>3</sup> h <sup>-1</sup> ) | 36.6                 | 34.7                 | 33.0                 | 30.0                 |
| Liquid flow rate $F_L$ (L h <sup>-1</sup> )           | 73.2                 | 182                  | 201                  | 360                  |
| $L/G$   | 1.5                  | 3.9                  | 4.7                  | 10.2                 |
| Gas velocity $U_G$ (m s <sup>-1</sup> )               | 0.90                 | 0.85                 | 0.81                 | 0.74                 |
| Liquid velocity $U_L$ (m s <sup>-1</sup> )            | $1.80 \cdot 10^{-3}$ | $4.47 \cdot 10^{-3}$ | $4.94 \cdot 10^{-3}$ | $8.84 \cdot 10^{-3}$ |

### 2.2. Chemical products

The physico-chemical properties of the three NAPLs are presented Table 2. The silicone oil used (polydimethylsiloxane, PDMS 20) was Rhodorsil 47V20 provided by Bluestar Silicones. The two waste oils were provided by Chimirec (Javené, France) (Lhuissier *et al.*, 2020).

Table 2: Characteristics of the solvents investigated.

|  | Tap water | PDMS 20   | Transformer oil | Lubricant |
|--|-----------|-----------|-----------------|-----------|
| Chemical composition                             |           | Siloxanes | Linear alkanes  |           |
| Dynamic viscosity $\mu_L$ (mPa s) at 25°C        | 0.889     | 20        | 19              | 79        |
| Molar mass (g mol <sup>-1</sup> )                | 18        | 3000      | 212             | 212       |
| Density $\rho_L$ (kg m <sup>-3</sup> )           | 997       | 900       | 865             | 875       |
| Surface tension $\sigma_L$ (mN m <sup>-1</sup> ) | 72        | 21        | 27              | 31        |

### 3. Results and discussion

#### 3.1. Removal efficiencies measurement

The experimental removal efficiencies ( $E_G$  defined according to Eq. 1) of the seven VOCs in the four different solvents are summarized in Tables 3-6.

$$E_G = \frac{C_{G,in} - C_{G,out}}{C_{G,in}} \quad \text{Equation 1}$$

$C_{G,in}$  and  $C_{G,out}$  are the inlet and the outlet VOC concentrations in the gas phase, respectively. On the one hand, removal efficiencies of the four non-polar VOCs (toluene, *m*-xylene, 1,3,5 TMB and n-heptane) in water were negligible whereas they were higher than 80% in transformer oil and PDMS 20. The removal efficiencies of these four VOCs were higher in the lubricant than in water but lower than in the transformer oil and PDMS 20, showing the detrimental influence of the solvent viscosity. With a moderate viscosity (around 19 mPa s) and a high affinity with most of the targeted VOCs, transformer oil exhibits slightly lower removal efficiencies than silicone oil (PDMS) owing to lower diffusivities. Given its lower CAPEX than PDMS, transformer oil would be a suitable liquid absorbent for an industrial application. On the other hand, removal efficiencies of the three more polar VOCs (ethyl acetate, MIBK and isopropanol) were in the range 78-99.9% in water (Table 6), and were in all cases better than in the three NAPLs, showing that water remains the most appropriate solvent to remove polar VOCs.

In order to rationalize these results, the absorption factor  $A$ , defined Eq. 2 (Biard *et al.*, 2017; Roustan, 2003), was calculated and the obtained values are summarized in Tables 3 to 6:

$$A = \frac{RTF_L}{H F_G} \quad \text{Equation 2}$$

$H$  (Pa m<sup>3</sup> mol<sup>-1</sup>) are the Henry's law constants of the solute/solvent systems extracted from the literature (Guillerm *et al.*, 2015; Lhuissier *et al.*, 2018; Staudinger and Roberts, 2001). Obviously,  $E_G$  increases with the absorption factor  $A$  for a given solvent (this behavior is easier to observe Fig. 4, which is introduced in Part 3.5). Thus,  $E_G$  values higher than 90% were measured in an only 1 m height column for the solvent/VOC couples characterized by an absorption factor  $A$  higher than 15-20. It confirms that the increase of the hydrophobic VOC/solvent affinity using NAPL is undoubtedly more beneficial than the lower mass transfer rate in the liquid phase caused by the higher viscosity. In order to treat efficiently a mixture of non-polar and polar VOCs, two packed columns in series, one fed with an NAPL and another one fed with water, would be a pertinent solution.

**Table 3: Values of the Henry's law constants  $H$  at 25°C (Lhuissier *et al.*, 2018), absorption factor  $A$  defined according to Eq. 2, experimental and modeled removal efficiencies  $E_G$ , experimental  $HTU_{OL}$  values, experimental and modeled  $K_L a^\circ$  values and relative mass transfer resistance in the liquid phase  $R_L$ , for the lubricant.  $RE$  corresponds to the relative error between the modeled and experimental values of  $E_G$  and  $K_L a^\circ$ . The adjusted SSR model corresponds to the SSR model (Eqs. 7-9) in which  $K_L a^\circ$  deduced from Eq. 4 is corrected with the correction factor  $C_1$  (part 3.4).**

| Solvent = lubricant    |                                     | Experimental results |                   |                           |            | SSR model           |                  |       |          | Adjusted SSR model  |                  |       |          |       |
|------------------------|-------------------------------------|----------------------|-------------------|---------------------------|------------|---------------------|------------------|-------|----------|---------------------|------------------|-------|----------|-------|
| Compound               | $H$                                 | $A$                  | $E_G \text{ exp}$ | $10^4 \times K_L a^\circ$ | $HTU_{OL}$ | $10^4 \times K_L a$ | $RE K_L a^\circ$ | $E_G$ | $RE E_G$ | $10^4 \times K_L a$ | $RE K_L a^\circ$ | $E_G$ | $RE E_G$ | $R_L$ |
|                        | Pa m <sup>3</sup> mol <sup>-1</sup> |                      |                   |                           |            |                     |                  |       |          |                     |                  |       |          |       |
| n-heptane              | 1.43                                | 3.47                 | 43.4%             | 3.18                      | 5.66       | 4.36                | 37.4%            | 53.5% | 23.3%    | 2.79                | 12.1%            | 39.6% | 8.8%     | 92.7% |
| Ethyl acetate          | 7.20                                | 0.69                 | 13.2%             | 4.12                      | 4.37       | 6.53                | 58.5%            | 19.1% | 44.7%    | 4.18                | 1.4%             | 13.4% | 1.2%     | 98.0% |
| Isopropanol            | 18.17                               | 0.27                 | ND                | ND                        | ND         | 8.13                | ND               | 9.5%  | ND       | 5.20                | ND               | 6.6%  | ND       | 99.1% |
| MIBK                   | 1.69                                | 2.93                 | ND                | ND                        | ND         | 5.13                | ND               | 52.7% | ND       | 3.28                | ND               | 39.1% | ND       | 92.9% |
| Toluene                | 0.71                                | 6.98                 | 73.3%             | 3.64                      | 4.94       | 5.08                | 39.7%            | 83.8% | 14.3%    | 3.25                | 10.6%            | 69.5% | 5.2%     | 83.4% |
| m-xylene               | 0.38                                | 13.0                 | 90.0%             | 3.33                      | 5.40       | 3.97                | 19.2%            | 93.5% | 3.9%     | 2.54                | 23.7%            | 82.9% | 7.9%     | 74.7% |
| 1,3,5-triméthylbenzène | 0.10                                | 49.6                 | 97.6%             | 1.37                      | 13.1       | 2.20                | 59.8%            | 99.7% | 2.2%     | 1.41                | 2.3%             | 97.8% | 0.2%     | 45.1% |

**Table 4: Values of the Henry's law constants  $H$  at 25°C (Lhuissier *et al.*, 2018), absorption factor  $A$  defined according to Eq. 2, experimental and modeled removal efficiencies  $E_G$ , experimental  $HTU_{OL}$  values, experimental and modeled  $K_L a^\circ$  values and relative mass transfer resistance in the liquid phase  $R_L$ , for the transformer oil.  $RE$  corresponds to the relative error between the modeled and experimental values of  $E_G$  and  $K_L a^\circ$ . The adjusted SSR model corresponds to the SSR model (Eqs. 7-9) in which  $K_L a^\circ$  deduced from Eq. 4 is corrected with the correction factor  $C_1$  (part 3.4).**

| Solvent = transformer oil |                                     | Experimental results |                   |                           |            | SSR model           |                  |        |          | Adjusted SSR model  |                  |       |          |       |
|---------------------------|-------------------------------------|----------------------|-------------------|---------------------------|------------|---------------------|------------------|--------|----------|---------------------|------------------|-------|----------|-------|
| Compound                  | $H$                                 | $A$                  | $E_G \text{ exp}$ | $10^4 \times K_L a^\circ$ | $HTU_{OL}$ | $10^4 \times K_L a$ | $RE K_L a^\circ$ | $E_G$  | $RE E_G$ | $10^4 \times K_L a$ | $RE K_L a^\circ$ | $E_G$ | $RE E_G$ | $R_L$ |
|                           | Pa m <sup>3</sup> mol <sup>-1</sup> |                      |                   |                           |            |                     |                  |        |          |                     |                  |       |          |       |
| n-heptane                 | 1.09                                | 11.9                 | 84.8%             | 7.41                      | 6.03       | 15.1                | 104%             | 97.7%  | 15.2%    | 9.68                | 30.5%            | 91.3% | 7.7%     | 70.2% |
| Ethyl acetate             | 4.69                                | 2.77                 | 48.0%             | 11.7                      | 3.82       | 27.1                | 132%             | 75.1%  | 56.5%    | 17.3                | 48.2%            | 60.7% | 26.5%    | 88.8% |
| Isopropanol               | 9.9                                 | 1.31                 | ND                | ND                        | ND         | 35.2                | ND               | 53.9%  | ND       | 22.5                | ND               | 41.7% | ND       | 93.7% |
| MIBK                      | 1.02                                | 12.74                | 82.2%             | 6.31                      | 7.08       | 16.7                | 164%             | 98.8%  | 20.3%    | 10.7                | 68.9%            | 94.4% | 14.8%    | 65.9% |
| Toluene                   | 0.50                                | 26.0                 | 88.8%             | 3.86                      | 11.6       | 12.9                | 235%             | 99.9%  | 12.5%    | 8.27                | 114%             | 99.1% | 11.5%    | 46.3% |
| m-xylene                  | 0.22                                | 59.1                 | 97.2%             | 2.75                      | 16.3       | 7.17                | 161%             | 100.0% | 2.8%     | 4.59                | 66.8%            | 99.7% | 2.6%     | 29.5% |
| 1,3,5-triméthylbenzène    | 0.13                                | 100                  | ND                | ND                        | ND         | 4.60                | ND               | 100.0% | ND       | 2.95                | ND               | 99.9% | ND       | 20.6% |

**Table 5: Values of the Henry's law constants  $H$  at 25°C (Guillerm *et al.*, 2015), absorption factor  $A$  defined according to Eq. 2, experimental and modeled removal efficiencies  $E_G$ , experimental  $HTU_{OL}$  values, experimental and modeled  $K_L a^\circ$  values and relative mass transfer resistance in the liquid phase  $R_L$ , for PDMS 20.  $RE$  corresponds to the relative error between the modeled and experimental values of  $E_G$  and  $K_L a^\circ$ . The adjusted SSR model corresponds to the SSR model (Eqs. 7-9) in which  $K_L a^\circ$  deduced from Eq. 4 is corrected with the correction factor  $C_1$  (part 3.4).**

| Solvent = PDMS 20      |                                     | Experimental results |                   |                           |            | SSR model           |                  |        |          | Adjusted SSR model  |                  |       |          |       |
|------------------------|-------------------------------------|----------------------|-------------------|---------------------------|------------|---------------------|------------------|--------|----------|---------------------|------------------|-------|----------|-------|
| Compound               | $H$                                 | $A$                  | $E_G \text{ exp}$ | $10^4 \times K_L a^\circ$ | $HTU_{OL}$ | $10^4 \times K_L a$ | $RE K_L a^\circ$ | $E_G$  | $RE E_G$ | $10^4 \times K_L a$ | $RE K_L a^\circ$ | $E_G$ | $RE E_G$ | $R_L$ |
|                        | Pa m <sup>3</sup> mol <sup>-1</sup> |                      |                   |                           |            |                     |                  |        |          |                     |                  |       |          |       |
| n-heptane              | 2.34                                | 6.45                 | 92.4%             | 22.0                      | 2.25       | 25.1                | 14.3%            | 94.7%  | 2.4%     | 16.1                | 26.9%            | 85.3% | 7.7%     | 77.4% |
| Ethyl acetate          | 6.39                                | 2.36                 | 74.5%             | 35.8                      | 1.38       | 40.4                | 12.9%            | 78.0%  | 4.8%     | 25.8                | 27.8%            | 64.3% | 13.6%    | 88.0% |
| Isopropanol            | 19.93                               | 0.76                 | 32.7%             | 34.4                      | 1.43       | 53.8                | 56.3%            | 42.0%  | 28.6%    | 34.4                | 0.0%             | 32.7% | 0.0%     | 95.3% |
| MIBK                   | 1.78                                | 8.48                 | 93.8%             | 17.6                      | 2.80       | 26.5                | 50.3%            | 98.4%  | 4.9%     | 16.9                | 3.9%             | 93.2% | 0.7%     | 69.7% |
| Toluene                | 2.15                                | 7.02                 | 97.1%             | 27.8                      | 1.78       | 30.0                | 8.2%             | 97.8%  | 0.7%     | 19.2                | 30.7%            | 91.7% | 5.6%     | 71.6% |
| m-xylene               | 0.71                                | 21.3                 | 98.4%             | 9.98                      | 4.94       | 17.5                | 75.3%            | 99.9%  | 1.5%     | 11.2                | 12.2%            | 99.0% | 0.6%     | 47.8% |
| 1,3,5-triméthylbenzène | 0.22                                | 68.6                 | ND                | ND                        | ND         | 7.73                | ND               | 100.0% | ND       | 4.95                | ND               | 99.9% | ND       | 23.0% |

**Table 6: Values of the Henry's law constants  $H$  at 25°C (Staudinger and Roberts, 2001), absorption factor  $A$  defined according to Eq. 2, experimental and modeled removal efficiencies  $E_G$ , experimental  $HTU_{OL}$  values, experimental and modeled  $K_L a^\circ$  values and relative mass transfer resistance in the liquid phase  $R_L$ , for water.  $RE$  corresponds to the relative error between the modeled and experimental values of  $E_G$  and  $K_L a^\circ$ . The adjusted SSR model corresponds to the SSR model (Eqs. 7-9) in which  $K_L a^\circ$  deduced from Eq. 4 is corrected with the correction factor  $C_1$  (part 3.4).**

| Solvent = water        |                                     | Experimental results  |                   |                           |            | SSR model           |                  |        |          | Adjusted SSR model  |                  |        |          |        |
|------------------------|-------------------------------------|-----------------------|-------------------|---------------------------|------------|---------------------|------------------|--------|----------|---------------------|------------------|--------|----------|--------|
| Compound               | $H$                                 | $A$                   | $E_G \text{ exp}$ | $10^4 \times K_L a^\circ$ | $HTU_{OL}$ | $10^4 \times K_L a$ | $RE K_L a^\circ$ | $E_G$  | $RE E_G$ | $10^4 \times K_L a$ | $RE K_L a^\circ$ | $E_G$  | $RE E_G$ | $R_L$  |
|                        | Pa m <sup>3</sup> mol <sup>-1</sup> |                       |                   |                           |            |                     |                  |        |          |                     |                  |        |          |        |
| n-heptane              | 2.08×10 <sup>5</sup>                | 1.43×10 <sup>-4</sup> | ND                | ND                        | ND         | 331                 | ND               | 0.0%   | ND       | 212                 | ND               | 0.0%   | ND       | 100.0% |
| Ethyl acetate          | 14.9                                | 2.00                  | 77.9%             | 90.1                      | 0.981      | 243                 | 170%             | 96.7%  | 24.1%    | 156                 | 72.6%            | 90.5%  | 16.2%    | 64.7%  |
| Isopropanol            | 0.31                                | 95.9                  | 99.9%             | 6.43                      | 13.8       | 15.0                | 133%             | 100.0% | 0.1%     | 9.57                | 49.0%            | 100.0% | 0.1%     | 3.7%   |
| MIBK                   | 21.1                                | 1.41                  | 79.6%             | 164                       | 0.540      | 253                 | 54%              | 88.4%  | 11.1%    | 162                 | 1.3%             | 79.3%  | 0.4%     | 72.0%  |
| Toluene                | 510                                 | 0.06                  | ND                | ND                        | ND         | 358                 | ND               | 5.7%   | ND       | 229                 | ND               | 5.3%   | ND       | 98.4%  |
| m-xylene               | 644.5                               | 0.05                  | ND                | ND                        | ND         | 341                 | ND               | 4.5%   | ND       | 218                 | ND               | 4.2%   | ND       | 98.7%  |
| 1,3,5-triméthylbenzène | 714.3                               | 0.04                  | ND                | ND                        | ND         | 331                 | ND               | 4.1%   | ND       | 212                 | ND               | 3.8%   | ND       | 98.8%  |

### 3.2. Calculation of the experimental $K_L a^\circ$ values

The experimental values of the overall volumetric mass transfer coefficients in the liquid phase  $K_L a^\circ$  were deduced from the experimental removal efficiencies  $E_G$  and the absorption factor  $A$  considering the HTU-NTU method considering gas and liquid plug-flows at counter-current and at steady-state (Biard *et al.*, 2018; Dumont, 2018; Rodriguez Castillo *et al.*, 2019).

$$K_L a^\circ = \frac{F_L}{S_{col} \times Z A - 1} \ln \left( \frac{A - E_G}{A(1 - E_G)} \right) \Leftrightarrow E_G = \frac{A \left( 1 - \exp \left( (1 - A) \frac{K_L a^\circ \times S_{col} \times Z}{F_L} \right) \right)}{A - \exp \left( (1 - A) \frac{K_L a^\circ \times S_{col} \times Z}{F_L} \right)} \Leftrightarrow Z = NTU_{OL} \times HTU_{OL}$$

$$\text{with } HTU_{OL} = \frac{F_L}{S_{col} \times K_L a^\circ} \text{ and } NTU_{OL} = \frac{1}{A - 1} \ln \left( \frac{A - E_G}{A(1 - E_G)} \right) \quad \text{Equation 3}$$

$S_{col}$  is the column cross-section ( $m^2$ ).  $K_L a^\circ$  depends on the local gas and liquid-side mass transfer coefficients ( $k_G$  and  $k_L$ ) and on the interfacial area according to Eq. 4:

$$K_L a^\circ = \left( \frac{1}{k_L} + \frac{RT}{Hk_G} \right)^{-1} a^\circ \quad \text{Equation 4}$$

$K_L a^\circ$  values have orders of magnitude of  $10^{-4}$  and  $10^{-3} \text{ s}^{-1}$  (Tables 3-6), consistent with those measured by Guillerm *et al.* (Guillerm *et al.*, 2016) and Heymes *et al.* (Frederic Heymes *et al.*, 2006) for the case of toluene absorption in silicone oil and DEHA, respectively. For the particular case of MIBK absorption in water,  $K_L a^\circ$  is even higher ( $1.64 \times 10^{-2} \text{ s}^{-1}$ ). To support the reliability of these values, a sensitivity analysis has been performed (Supplementary material, Fig. S.1(b) to Fig. S.3(b)) through the calculation of the elasticity indexes relative to the output  $K_L a^\circ$ . Both the absorption factor  $A$  and the measured gas concentration (which influences directly the values of  $E_G$  measured according to Eq. 1) were considered as the inputs. The elasticity indexes were evaluated for  $H$  values lower than 20 in agreement with the values reported in Tables 3 to 6. The results show that the values of  $K_L a^\circ$  determined are poorly sensitive to the values of  $A$  (*i.e.* to the values of  $F_L$ ,  $F_G$  and  $H$  according to Eq. 2) taken into account when applying Eq. 3, with corresponding elasticity indexes lower than 2. Thus, even if the values of  $H$  considered could be affected by experimental uncertainties, their influence remains limited. The sensitivity to the measured gas concentration (*i.e.* to the removal efficiency) is more significant for the specific case of the lubricant. Nonetheless, only point (corresponding to ethyl acetate removal in the lubricant) was determined at a high value of  $H$  (7.20), with a corresponding elasticity index of around 7.2. Thus, only in that

case, a significant experimental uncertainty on the measured value of  $E_G$  can affect the value of  $K_L a^\circ$  with a great extent. All the other values of  $K_L a^\circ$  should be reliable.

In agreement with Eq. 4,  $K_L a^\circ$  decreases with the Henry's law constant  $H$ . At similar values of  $H$ ,  $K_L a^\circ$  decreases also with the dynamic viscosity  $\mu_L$ , which is clearly emphasized by the data relative to the lubricant (Table 3). Indeed, a higher viscosity increases the mass transfer resistance in the liquid phase, directly through lower turbulences and indirectly through lower diffusivities (Rodriguez Castillo *et al.*, 2019; Song *et al.*, 2018, 2014). Besides, at similar values of  $H$  and of the viscosity  $\mu_L$ ,  $K_L a^\circ$  values are slightly lower in transformer oil than in PDMS 20, which might be justified by the influence of  $D_L$ , the diffusivity in the liquid phase (Table A.1 in appendix). The lower diffusivities in the waste oils are induced by their low molar volumes (Rodriguez Castillo *et al.*, 2019). In order to address more extensively the influence of the solvent viscosity and of the diffusivity on the overall mass transfer coefficients, a deconvolution procedure is developed part 3.3.

### 3.3. Deconvolution procedure using the Higbie penetration theory

#### 3.3.1. Step 1: Calculation of the interfacial area

Table 7: Semi-empirical correlations for the determination of the interfacial area  $a^\circ$  and of the local mass transfer coefficients  $k_L$  and  $k_G$  in counter-current packed column.

| Model  | Correlation   | Eq. number |
|--|---|------------|
| <b>BS (Billet and Schultes, 1999, 1993b)</b>                             | $a^\circ$ calculation requires beforehand calculation of the loading and flooding points and of the liquid holdup $h_L$ (Table 4 in (Lhuissier <i>et al.</i> , 2020)). Determined for $0.74 \times 10^{-6} \leq \mu_L / \rho_L \leq 142 \times 10^{-6} \text{ m}^2 \text{ s}^{-1}$                                    |            |
|  | $k_L = C_L \times 12^{1/6} \times \left( \frac{U_L}{h_L} \right)^{0.5} \times \left( \frac{D_L}{d_h} \right)^{0.5}$<br>Determined for $0.14 \times 10^{-6} \leq \mu_L / \rho_L \leq 1.66 \times 10^{-6} \text{ m}^2 \text{ s}^{-1}$   | Equation 5 |
|  | $k_G = C_V \times \frac{1}{(\varepsilon - h_L)^{0.5}} \frac{A_p^{0.5}}{d_h^{0.5}} \times D_G \times \left( \frac{\rho_G U_G}{A_p \mu_G} \right)^{0.75} \left( \frac{\mu_G}{\rho_G D_G} \right)^{1/3}$<br>Determined for $0.14 \times 10^{-6} \leq \mu_L / \rho_L \leq 1.66 \times 10^{-6} \text{ m}^2 \text{ s}^{-1}$ | Equation 6 |
| <b>SSR (Song <i>et al.</i>, 2018)</b>                                    | $\frac{a_0}{A_p} = 1.16 \times \eta \times \left( \left( \frac{\rho_L}{\sigma_L} \right) \times g^{0.5} \times U_L \times A_p^{-1.5} \right)^{0.138}$   | Equation 7 |
| <b>Determined for <math>0.80 \leq \mu_L \leq 70 \text{ mPa s}</math></b> | $\eta = 1.15$ for a structured packing in steel operated in the loading zone  |            |
|  | $k_L = 0.12 \times U_L^{0.565} \left( \frac{\mu_L}{\rho_L} \right)^{-0.40} D_L^{0.5} g^{1/6} A_p^{-0.065} \left( \frac{Z}{1.8} \right)^{-0.54}$   | Equation 8 |
|  | $k_G = 0.28 \times U_G^{0.62} \left( \frac{\mu_G}{\rho_G} \right)^{-0.12} D_G^{0.5} A_p^{0.38} \sin(2\alpha)$<br>$\alpha$ is the corrugation angle (here $45^\circ$ )   | Equation 9 |

In this study, the selected gas and liquid flow rates, and consequently the interfacial area  $a^\circ$ , were unchanged for a given solvent. Thus, for each solvent, only the overall mass transfer coefficient  $K_L$  is expected to vary with the nature of the VOC (through the variations of  $H$ ,  $D_L$  and  $D_G$ ).

Two models have been considered to estimate the values of  $a^\circ$  (Table 7). These models were developed for both random and structured packing, and not only for water-like solvents:

- The Billet-Schultes correlations were developed in the nineties (Billet and Schultes, 1999, 1993b). These correlations require the use of several constants specific of the selected packing ( $C_V$  and  $C_L$ ). Besides, the loading and flooding points have to be determined beforehand by numerical resolution (Billet and Schultes, 1999; Lhuissier *et al.*, 2020). According to this model, the liquid holdup  $h_L$ , and consequently the interfacial area  $a^\circ$ , depend significantly on the solvent viscosity.
- The Song-Seibert-Rochelle correlation (Song *et al.*, 2018) was developed a few years ago particularly for viscous solvents up to 70 mPa s. This model presents the advantage to be easy to implement, with no packing-specific constant required. The authors tested 39 different random or structured packings in various materials (stainless steel or plastic). Contrarily to the observations of Billet-Schultes, they concluded that the interfacial area does not depend significantly on the liquid viscosity (unlike to the liquid holdup) (Song *et al.*, 2018).

Table 8 summarizes the interfacial area calculated with the two models. A significant deviation between them is observed, especially for water, which would exhibit a significantly lower interfacial area  $a^\circ$  according to the BS model (around three times).

**Table 8: Interfacial area  $a^\circ$  ( $\text{m}^2 \text{m}^{-3}$ ) calculated with the BS and SSR models and of the liquid holdup ( $h_L$ ). The values of the BS model results are taken into account as the reference to calculate the relative error (RE).**

|                 | $10^6 \times \mu_L / \rho_L$ ( $\text{m}^2 \text{s}^{-1}$ ) | BS    |                               | SSR                           | RE   |
|-----------------|---|-------|-------------------------------|-------------------------------|------|
|                 |   | $h_L$ | $a^\circ$ ( $\text{m}^{-1}$ ) | $a^\circ$ ( $\text{m}^{-1}$ ) |      |
| Lubricant       | 90.3  | 0.335 | 523                           | 371                           | 29%  |
| Transformer oil | 22.0  | 0.476 | 788                           | 428                           | 45%  |
| PDMS            | 22.2  | 0.434 | 745                           | 452                           | 39%  |
| Water           | 0.89  | 0.186 | 114                           | 419                           | 267% |

### 3.3.2. Step 2: determination of the renewal times $\tau_L$ and $\tau_G$ at the interface according to the Higbie penetration theory

According to Eq. 4,  $K_L$  depends only the Henry's law constant  $H$  and the local mass transfer coefficients  $k_L$  and  $k_G$ , which depend respectively on liquid and gas diffusivities  $D_L$  and  $D_G$ . According to the Higbie penetration theory (Higbie, 1935), the gas-liquid interface consists of liquid and gas infinitesimal elements continuously renewed at the surface. Furthermore, local mass transfer coefficients are directly proportional to the square root of the diffusivities and  $\tau_L$  and  $\tau_G$ , the renewal times of the liquid and gas elements at the gas-liquid interface:

$$k_L = \sqrt{\frac{4 \cdot D_L}{\pi \tau_L}} \quad \text{Equation 10}$$

$$k_G = \sqrt{\frac{4 D_G}{\pi \tau_G}} \quad \text{Equation 11}$$

Then, from Eqs. 4, 10 and 11, Eq. 12 is obtained (Biard *et al.*, 2016):

$$\frac{\sqrt{\frac{4 \cdot D_L}{\pi}}}{K_L} = \sqrt{\tau_L} + \sqrt{\tau_G} \frac{R \cdot T}{H} \sqrt{\frac{D_L}{D_G}} \quad \text{Equation 12}$$

The values of  $K_L$  were deduced from the  $K_L a^\circ$  experimental values divided by the interfacial area  $a^\circ$  previously calculated using both the BS and SSR models (Table 8). The values of  $D_L$  and  $D_G$  computed are summarized in appendix (Table A.1). The correlations of the literature are rather inaccurate for the calculation of  $D_L$  in viscous solvents (Biard *et al.*, 2016; Bourgois *et al.*, 2008; Hadjoudj *et al.*, 2008; Rodriguez Castillo *et al.*, 2019). Consequently, two correlations were considered for the sake of comparison, the well-known correlation of Wilke-Chang and the correlation of Rodriguez *et al.* developed with ionic liquids having viscosities around 50 mPa s (Perry and Green, 1997; Rodriguez Castillo *et al.*, 2019; Roustan, 2003).

Thus, Fig. 1 represents the dependence of  $\frac{\sqrt{\frac{4 \cdot D_L}{\pi}}}{K_L}$  on  $\frac{RT}{H} \sqrt{\frac{D_L}{D_G}}$  considering both the Wilke-Chang and Rodriguez *et al.* correlations for  $D_L$  and both the BS and SSR correlations for  $a^\circ$  (four methods). As expected, linear relationships are obtained even if a significant dispersion of the points attributed to the experimental uncertainties on  $E_G$  (and then on  $K_L a^\circ$ ) and on the computed values of  $H$ , is observed (See the sensitivity analysis, in the part 1 of the

supplementary material). Then, values of  $\sqrt{\tau_L}$  and  $\sqrt{\tau_G}$  were deduced for each solvent and each method from the y-intercept and the slope, respectively (Table 9).

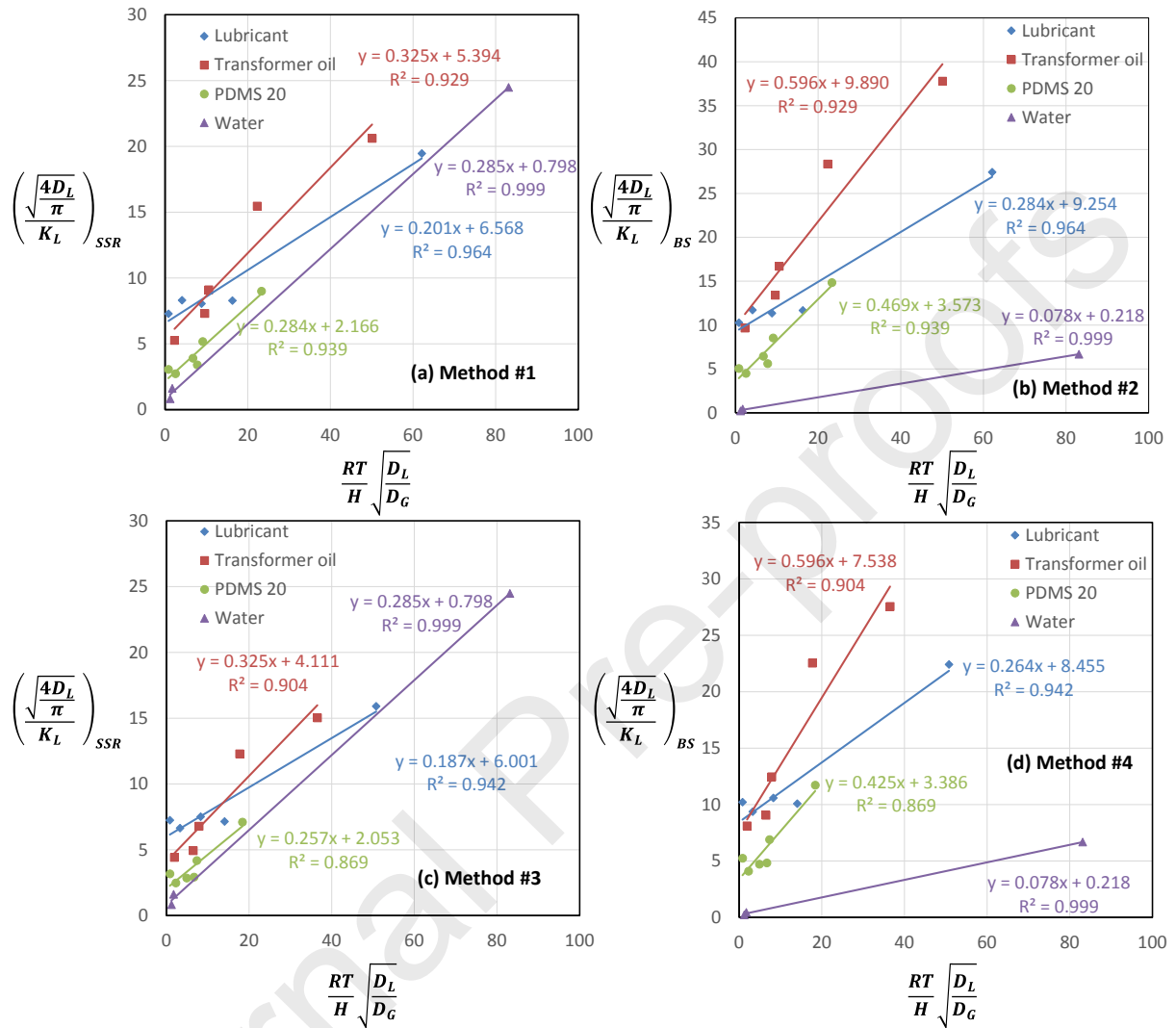


Figure 1:  $\frac{\sqrt{4D_L}}{\pi} / K_L$  as a function of  $\frac{RT}{H} \sqrt{\frac{D_L}{D_G}}$  for the four solvents. (a): Method #1,  $D_L$  from Rodriguez *et al.* and  $\alpha^\circ$  from SSR model. (b): Method #2,  $D_L$  from Rodriguez *et al.* and  $\alpha^\circ$  from BS model. (c): Method #3,  $D_L$  from Wilke-Chang and  $\alpha^\circ$  from SSR model. (d): Method #4,  $D_L$  from Wilke-Chang and  $\alpha^\circ$  from BS model.

**Table 9: Values of  $\sqrt{\tau_L}$  and  $\sqrt{\tau_G}$  (in  $s^{1/2}$ ) determined from Fig. 1. Values in bold will be used to determine the experimental values of  $k_L$  and  $k_G$  (part 3.3.4)**

|                        | Method #1<br>$D_L$ from Wilke-<br>Chang<br>$\alpha^\circ$ from SSR |                | Method #2<br>$D_L$ from Wilke-<br>Chang<br>$\alpha^\circ$ from BS |                | Method #3<br>$D_L$ from Rodriguez <i>et al.</i><br>$\alpha^\circ$ from SSR |                | Method #4<br>$D_L$ from Rodriguez <i>et al.</i><br>$\alpha^\circ$ from BS |                |
|------------------------|--|----------------|---|----------------|--|----------------|---|----------------|
|                        | $\tau_G^{0.5}$   | $\tau_L^{0.5}$ | $\tau_G^{0.5}$  | $\tau_L^{0.5}$ | $\tau_G^{0.5}$   | $\tau_L^{0.5}$ | $\tau_G^{0.5}$  | $\tau_L^{0.5}$ |
| <b>Lubricant</b>       | 0.201  | 6.57           | 0.284   | 9.25           | <b>0.187</b>   | <b>6.00</b>    | 0.264   | 8.46           |
| <b>Transformer oil</b> | 0.325  | 5.39           | 0.596   | 9.89           | <b>0.325</b>   | <b>4.11</b>    | 0.596   | 7.36           |
| <b>PDMS 20</b>         | 0.284  | 2.17           | 0.469   | 3.57           | <b>0.257</b>   | <b>2.05</b>    | 0.425   | 3.39           |
| <b>Water</b>           | 0.285  | 0.798          | 0.0780  | 0.218          | <b>0.285</b>   | <b>0.798</b>   | 0.0780  | 0.218          |

On the one hand, Table 9 clearly shows that the influence of the correlations used to calculate  $D_L$  is low. In this case, the average relative errors (ARE) relative to  $\sqrt{\tau_L}$  and  $\sqrt{\tau_G}$  are 5.7% and 14%, respectively (ARE is calculated by comparing the values of Method #1 to the values of #3 and by comparing the values of Method #2 to the values #4). On the other hand, the influence of the model considered to estimate  $\alpha^\circ$  (BS or SSR model) is particularly high (Method #1 vs. Method #2 and Method #3 vs. Method #4), which was expected regarding the significant differences of  $\alpha^\circ$  values predicted by the two models (Table 8). Considering the BS model, very different values of  $\sqrt{\tau_G}$  are found (Method #2 and Method #4), which is unlikely considering that the gas velocities were quite similar from one solvent to another (Table 3).  $\sqrt{\tau_L}$  increased with the solvent viscosity (except with the Method #2), in agreement with an expected higher renewal time of liquid elements at the liquid-gas interface due to lower turbulences. Thus, the SSR might appear as more accurate. Nonetheless, a deeper analysis (part 3.3.3, step 3) is required to quantify the real influence of the solvent viscosity on the mass transfer resistance in the liquid phase and to assess which model (among the BS and SSR models) better considers this effect.

### 3.3.3. Step 3: evaluation of the reliability of $\tau_L$ values with BS and SSR models

The correlations of BS and SSR to calculate  $k_L$  and  $k_G$  are summarized Table 7.

- According to the SSR model (Eq. 8),  $k_L \propto U_L^{0.565} \mu_L^{-0.40} \rho_L^{0.40} D_L^{0.5}$ . According to Eq. 10, it leads to:

$$\ln(\tau_L^{0.5} U_L^{0.565} \rho_L^{0.40}) \propto 0.40 \ln(\mu_L) \quad \text{Equation 13}$$

- According to the BS model (Eq. 5),  $k_L \propto U_L^{0.5} h_L^{-0.5} D_L^{0.5}$ . According to Eq. 10, it leads to:

$$\ln(\tau_L^{0.5} U_L^{0.5}) \propto 0.50 \ln(h_L) \quad \text{Equation 14}$$

Thus, taking into account the four values of  $\tau_L$  found (Methods #1 to #4, Table 9),  $\ln(\tau_L^{0.5} U_L^{0.565} \rho_L^{0.40})$  was plotted against  $\ln(\mu_L)$  (Fig. 2) and  $\ln(\tau_L^{0.5} U_L^{0.5})$  was plotted against  $\ln(h_L)$  (Fig. 3). Each point corresponds to one solvent. Whatever the method used to determine  $\tau_L$  (Table 9), the proportionality between  $\ln(\tau_L^{0.5} U_L^{0.5})$  and  $h_L$  ( $h_L$  is determined with the BS model) is low (Fig. 3). Furthermore, the slopes of the linear regression applied (from 1.13 to 3.39) are far from the expected value of 0.50 (Eq. 14). Indirectly, it means that the BS model badly correlates  $k_L$  and  $\tau_L$  to the viscosity. On the contrary, the linearity is better when  $\ln(\tau_L^{0.5} U_L^{0.565} \rho_L^{0.40})$  is plotted against  $\ln(\mu_L)$  (Fig. 2), even if a dispersion of the points relative to transformer and silicone oils is observed. Furthermore, when  $a^\circ$  is calculated with the SSR model (Methods #1 and #3, red triangles and green diamonds, respectively), the slopes (0.44 when  $D_L$  is estimated with the Rodriguez *et al.* correlation, 0.47 when  $D_L$  is estimated with the Wilke-Chang correlation) are close to the expected values of 0.40 (Eq. 13). It shows that the SSR model for the prediction of both  $k_L$  and  $a^\circ$  (Eq. 8 and 9) correlates accurately the experimental data to the solvents and solutes properties ( $H$ ,  $D_L$ ,  $D_G$  and more particularly the solvent viscosity  $\mu_L$ ). Contrarily to the BS model, the SSR model was entirely built using solvents with viscosities up to 70 mPa s, covering the range of viscosity of the solvents used (Tables 2 and 7). The influence of the considered correlation used to calculate  $D_L$  is limited on Fig. 2. However, using the correlation of Rodriguez *et al.*, a better determination coefficient ( $R^2 = 0.89$ ; green points) and a slope of 0.44 closer to the expected value of 0.40 are obtained. Thus, the values of  $\tau_L$  and  $\tau_G$  determined with the Method #3 (Table 9) will be considered in the part 3.3.4 to calculate the experimental values of  $k_L$  and  $k_G$ .

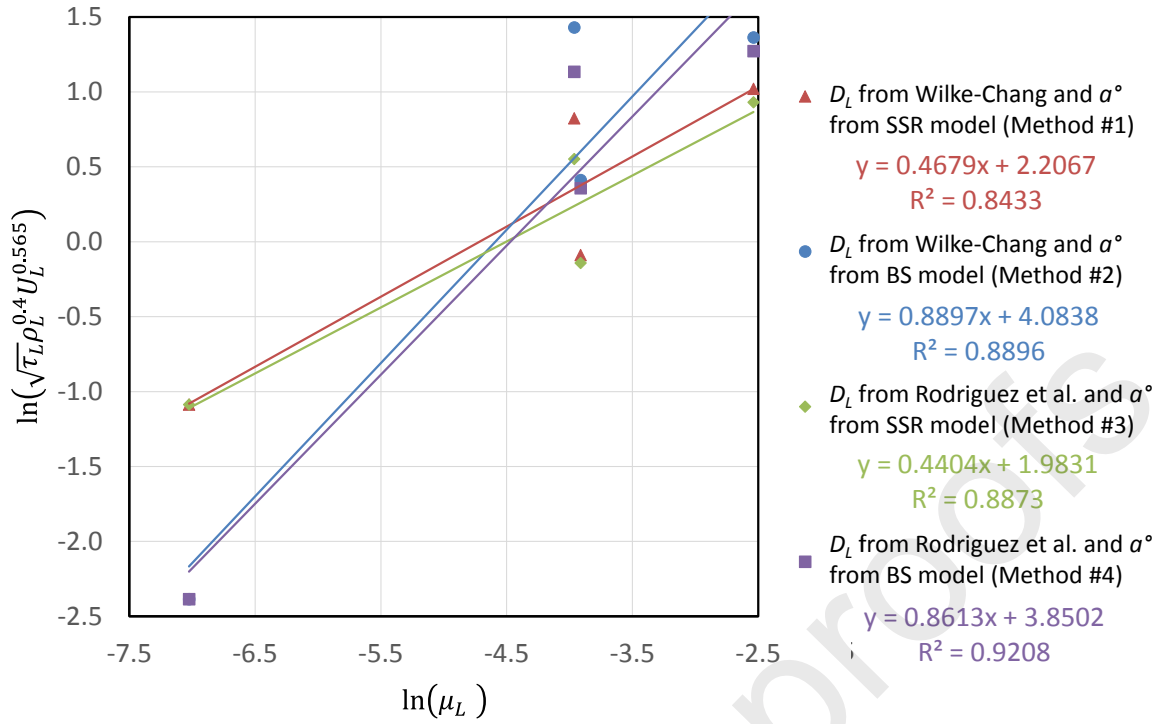


Figure 2:  $\ln(\tau_L^{0.5} U_L^{0.565} \rho_L^{0.40})$  as a function of  $\ln(\mu_L)$  taking the values of  $\tau_L$  summarized Table 9 into account.

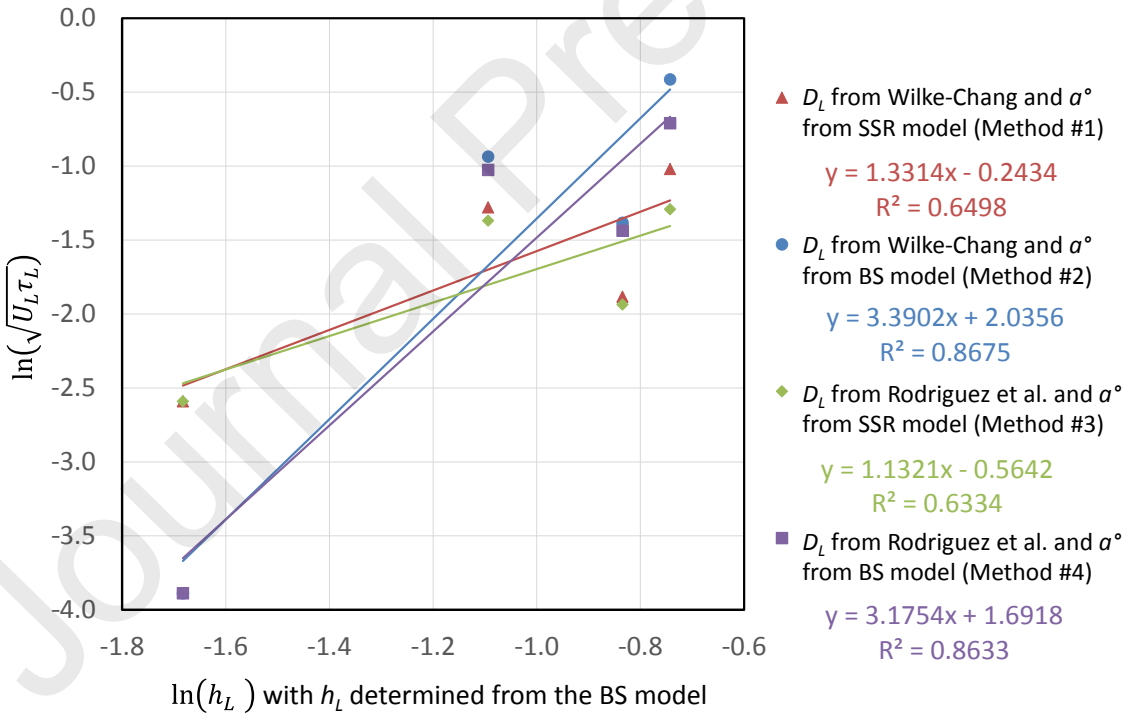


Figure 3:  $\ln(\tau_L^{0.5} U_L^{0.5})$  as a function of  $\ln(h_L)$  taking the values of  $\tau_L$  summarized Table 9 into account.

3.3.4. Step 4: Determination of the experimental local mass transfer coefficients  $k_L$  and  $k_G$ 

Table 10: Local liquid-side and gas-side mass transfer coefficients  $k_L$  and  $k_G$  gathered from the experiments ( $\alpha^\circ$  from the SSR model and  $D_L$  from the Rodriguez *et al.* correlation) and comparison to the predictions of the BS (with  $C_V = 0.109$  and  $C_L = 0.355$ ) and SSR models.

| Solvent       | VOC             | Experimental                           |  | BS model (Eqs 5 & 6)                   |  | SSR model (Eqs 8 & 9)                  |  |
|---------------|-----------------|--|--|--|--|--|--|
|               |                 | $10^2 \times k_G$<br>m s <sup>-1</sup> | $10^6 \times k_L$<br>m s <sup>-1</sup> | $10^2 \times k_G$<br>m s <sup>-1</sup> | $10^6 \times k_L$<br>m s <sup>-1</sup> | $10^2 \times k_G$<br>m s <sup>-1</sup> | $10^6 \times k_L$<br>m s <sup>-1</sup> |
| Lubricant     | n-heptane       | 1.60                                   | 1.01                                   | 1.15                                   | 2.28                                   | 2.78                                   | 1.27                                   |
|               | Ethyl acetate   | 1.78                                   | 1.43                                   | 1.33                                   | 3.22                                   | 3.09                                   | 1.79                                   |
|               | Isopropanol     | 1.93                                   | 1.76                                   | 1.48                                   | 3.97                                   | 3.35                                   | 2.21                                   |
|               | MIBK            | 1.65                                   | 1.19                                   | 1.20                                   | 2.67                                   | 2.87                                   | 1.49                                   |
|               | Toluene         | 1.66                                   | 1.31                                   | 1.21                                   | 2.95                                   | 2.88                                   | 1.64                                   |
|               | m-xylene        | 1.59                                   | 1.14                                   | 1.14                                   | 2.57                                   | 2.76                                   | 1.43                                   |
|               | TMB             | 1.54                                   | 1.05                                   | 1.09                                   | 2.36                                   | 2.67                                   | 1.31                                   |
|               | Transformer oil | n-heptane                              | 0.92                                   | 4.74                                   | 1.26                                   | 4.53                                   | 2.69                                   |
| Ethyl acetate | 1.02            | 6.71                                   | 1.45                                   | 6.41                                   | 2.99                                   | 7.12                                   |  |
| Isopropanol   | 1.11            | 8.27                                   | 1.62                                   | 7.90                                   | 3.24                                   | 8.78                                   |  |
| MIBK          | 0.95            | 5.56                                   | 1.31                                   | 5.31                                   | 2.77                                   | 5.91                                   |  |
| Toluene       | 0.95            | 6.15                                   | 1.32                                   | 5.87                                   | 2.78                                   | 6.52                                   |  |
| m-xylene      | 0.92            | 5.36                                   | 1.25                                   | 5.12                                   | 2.67                                   | 5.69                                   |  |
| TMB           | 0.88            | 4.91                                   | 1.20                                   | 4.69                                   | 2.58                                   | 5.22                                   |  |
| PDMS 20       | n-heptane       | 1.17                                   | 8.11                                   | 1.17                                   | 8.11                                   | 2.61                                   | 7.18                                   |
|               | Ethyl acetate   | 1.29                                   | 11.5                                   | 1.34                                   | 11.5                                   | 2.90                                   | 10.1                                   |
|               | Isopropanol     | 1.41                                   | 14.1                                   | 1.50                                   | 14.1                                   | 3.14                                   | 12.5                                   |
|               | MIBK            | 1.20                                   | 9.50                                   | 1.21                                   | 9.50                                   | 2.69                                   | 8.41                                   |
|               | Toluene         | 1.21                                   | 10.5                                   | 1.22                                   | 10.5                                   | 2.70                                   | 9.29                                   |
|               | m-xylene        | 1.16                                   | 9.15                                   | 1.16                                   | 9.15                                   | 2.59                                   | 8.10                                   |
|               | TMB             | 1.12                                   | 8.39                                   | 1.10                                   | 8.39                                   | 2.50                                   | 7.43                                   |
|               | Water           | n-heptane                              | 1.05                                   | 102                                    | 0.89                                   | 36.5                                   | 2.46                                   |
| Ethyl acetate |                 | 1.17                                   | 116                                    | 1.03                                   | 41.4                                   | 2.73                                   | 89.8                                   |
| Isopropanol   |                 | 1.27                                   | 125                                    | 1.14                                   | 44.8                                   | 2.96                                   | 97.0                                   |
| MIBK          |                 | 1.08                                   | 108                                    | 0.93                                   | 38.7                                   | 2.53                                   | 83.7                                   |
| Toluene       |                 | 1.09                                   | 112                                    | 0.93                                   | 40.1                                   | 2.54                                   | 86.9                                   |
| m-xylene      |                 | 1.04                                   | 106                                    | 0.88                                   | 38.1                                   | 2.44                                   | 82.6                                   |
| TMB           |                 | 1.01                                   | 103                                    | 0.84                                   | 36.9                                   | 2.36                                   | 80.0                                   |

Taking into account the  $D_L$  values calculated with the Rodriguez *et al.* correlation and the  $D_G$  values (Table A.1),  $k_L$  and  $k_G$  (Table 10) were calculated according to Eqs 10 and 11 with the values of  $\tau_G$  and  $\tau_L$  determined with Method #3 (Table 9). On the one hand,  $k_G$  values are in a narrow range, from 0.0089 m s<sup>-1</sup> (n-heptane in water) to 0.0192 m s<sup>-1</sup> (isopropanol in lubricant), consistent with the order of magnitude usually observed in packed column (Rodriguez Castillo *et al.*, 2019). The values of  $k_G$  depends on the nature of the solvent only because slightly different gas superficial velocities were used. On the other hand,  $k_L$  values are stretched on two orders of magnitude, from  $1.01 \times 10^{-6}$  (n-heptane in lubricant) to  $1.25 \times 10^{-4}$  m s<sup>-1</sup> (isopropanol in water), highlighting the influence of the solvent viscosity  $\mu_L$  on  $k_L$  through its impact on both  $D_L$  and on the liquid phase turbulence. Thus, particularly low values of  $k_L$  are obtained in viscous solvents. For a given solvent, the slight dispersion of the

values of  $k_L$  and  $k_G$  are only due to the small variations of  $D_L$  and  $D_G$  respectively. In the part 3.4, these experimental values of  $k_L$  and  $k_G$  are compared to the values predicted by the BS and SSR models (Table 7).

### 3.4. Comparison between experimental and predicted $k_L$ and $k_G$ values

#### 3.4.1. SSR model assessment

SSR model (Song *et al.*, 2018) is particularly appealing owing to its easy application. Developed for viscous solvents, it does not require any packing-dependent or fluid-dependent constant. Besides, according to the part 3.3.3, it accurately describes the influence of the viscosity on  $k_L$  and  $a^\circ$ . Table 10 shows that the orders of magnitude of  $k_L$  and  $k_G$  predicted by the model are consistent with the experimental values. The values of  $D_L$  calculated with the Rodriguez *et al.* correlation were used (Table A.1). On the one hand,  $k_L$  values are well predicted by the model with an *ARE* of 16%: they are overestimated by the model by 25% and 6% for the lubricant and the transformer oil, respectively, and are underestimated by the model by 11% and 22% for PDMS 20 and water, respectively. On the other hand, the model overestimates  $k_G$  more than twice (*ARE* = 131%). Taking into account these modeled values of  $k_L$  and  $k_G$ ,  $K_L a^\circ$  values were calculated according to Eq. 4 and are summarized in Tables 3-6. In this case, modeled  $K_L a^\circ$  values calculated according to Eq. 3 are overestimated with an *ARE* of 83% (Tables 3-6). Indeed, except in few cases (non-polar VOCs absorption in water), the resistance in the gas phase cannot be neglected and the errors on the determined  $k_G$  values affect significantly  $K_L a^\circ$ . Actually,  $R_L$ , the relative resistance in liquid phase calculated according to Eq. 15 (Biard *et al.*, 2018), is not equal to one, contrary to the intuition which could suggest that the whole mass-transfer resistance might be located in the liquid phase using viscous solvents.

$$R_L = \left(1 + \frac{RTk_L}{k_G}\right)^{-1} \quad \text{Equation 15}$$

More precisely,  $R_L$  is in the range from 21 to 99% in the three NAPLs (Tables 3-5). In water,  $R_L$  tends toward one only for the non-polar VOCs, showing that for these specific cases, which would be unsuitable for industrial applications, the mass-transfer resistance might be entirely located in the liquid-phase (Table 6).

To improve the reliability of the SSR model, a correction factor  $C_1$  was applied to the  $K_L a^\circ$  values determined by the SSR model (adjusted SSR model). The value of  $C_1$  (= 0.640) was determined by minimizing the sum of the relative errors between the experimental and modeled values of  $K_L a^\circ$ . With this correction factor, *ARE* between

the experimental and modeled  $K_L a^\circ$  values climbed to 32% (Tables 3-6). The parity plots relative to  $K_L a^\circ$  between the SSR and adjusted SSR models are presented as supplementary material (Fig S.4). It shows that the influence of the viscosity is well taken into account by the SSR model, in agreement with the analysis of the part 3.3.3, and that the adjusted SSR model fits well to the experimental data. The dispersion of the points is justified by the experimental uncertainties on the determined removal efficiencies but also on the Henry's law constant values  $H$  extracted from the literature (Guillerm *et al.*, 2015; Lhuissier *et al.*, 2018; Staudinger and Roberts, 2001), which were used to determine the experimental values of  $K_L a^\circ$  (part 3.2), in agreement with the sensitivity analysis (Figs. S1(b) to S3 (b)).

### 3.4.2. BS model assessment

Billet-Schultes model requires beforehand to calculate the liquid holdup (Table 8) following the set of equations that they developed (Billet and Schultes, 1999, 1993b). Besides, the two packing-dependent constants  $C_L$  and  $C_V$ , unknown for the studied packing, have been determined ( $C_L = 0.355$  and  $C_V = 0.109$ ) by trying to minimize the sum of the relative errors between the experimental and modeled values of  $k_L$  and  $k_G$ . ARE between the experimental and modeled values of  $k_L$  and  $k_G$  were respectively equal to 40% and 20% (Table 10).  $C_L$  and  $C_V$  values were significantly lower than the ranges determined by Billet and Schultes for other packings, particularly  $C_L$  (the lowest values of  $C_L$  and  $C_V$  determined by BS are respectively 0.739 and 0.167 (Billet and Schultes, 1999)).

With this value of  $C_L$ , the values of  $k_L$  for the transformer oil and the lubricant (the solvents with intermediate viscosities) are well estimated, but the values for the lubricant and water are clearly overestimated (by a factor 2.25) and underestimated (by a factor 2.79), respectively. Here, the proposed value of  $C_L$  was optimized taking into account the four solvents. Nonetheless by considering each solvent independently, increasing values of  $C_L$  with the viscosity were found ( $C_L = 0.157$  considering lubricant to 0.991 considering water). This observation, in agreement with the analysis performed part 3.3.3 (Fig. 3), confirms that the model cannot predict accurately the influence of the viscosity on  $k_L$  and/or on  $h_L$ . The BS model relative to mass transfer coefficients determination was developed with solvents having kinematic viscosities in the range from 0.14 to  $1.66 \times 10^{-6} \text{ m}^2 \text{ s}^{-1}$ , which includes only water among the four tested solvents (Billet and Schultes, 1999). The kinematic viscosities of the three NAPLs are one order of magnitude higher (Table 8), from  $2.2 \times 10^{-5}$  (silicone and transformer oils) to  $9.0 \times 10^{-5} \text{ m}^2 \text{ s}^{-1}$  (lubricant); thus, such a discrepancy is not surprising. Therefore, only the SSR model is taken into account in the next part to model the removal efficiency.

### 3.5. Calculation of the removal efficiency $E_G$

From the previously calculated values of  $K_L a^\circ$  (Tables 3-6), removal efficiencies  $E_G$  were calculated taking into account the original SSR model and the adjusted SSR model. The original SSR model slightly overestimates  $E_G$  with an *ARE* of 14%, in agreement with overestimated  $K_L a^\circ$  values (*ARE* of 83%, part 3.4.1). Using the adjusted SSR model, no tendency to overestimate or underestimate  $E_G$  compared to the experimental values is observed, with an *ARE* of 7%. The parity plots are provided as supplementary material (Fig S.5). Thus, even with the original SSR model, a satisfactory agreement can be obtained, owing to the fact that the removal efficiency has a rather low sensitivity to  $K_L a^\circ$  as demonstrated by the sensitivity analysis provided in the supplementary material (Fig. S.1(a) to S.3(a)), with corresponding elasticity indexes in the range from 0.01 to 0.80, depending on  $H$ . Indeed, the sensitivity of the output  $E_G$  to the input  $K_L a^\circ$  is low with elasticity indexes lower than 1 whatever the solvent considered. Furthermore, the sensitivity to the Henry's law constant  $H$ , and so to the absorption factor  $A$ , is also characterized by elasticity indexes lower than one. Nonetheless, contrarily to  $K_L a^\circ$  values, which remain in a narrow range for a given solvent,  $H$  values can vary over several orders of magnitude. Fig. 4 shows  $E_G$  dependence (calculated with the adjusted SSR model) on the absorption factor  $A$  for the various VOC/solvent systems. It shows that  $E_G$  higher than 90% is obtained when  $A$  is higher than 20, whatever the solvent. Using viscous solvents, low loading and flooding points are involved, requiring to operate at low  $L/G$  ratio (Lhuissier *et al.*, 2020) meaning that  $A$  higher than 20 would be only feasible for low values of  $H$  (*i.e.* high affinity between solute and solvent). For values of  $A$  lower than 20,  $E_G$  is more sensitive to solvent viscosity. This behavior is easier to observe in Fig. S.6 provided as supplementary material, in which average values of  $k_L$  and  $k_G$  (from Table 10) were considered for each solvent to avoid the slight dispersion of the points related to small variations of  $D_L$  and  $D_G$  for the different VOCs. For example, for  $A = 2$ ,  $E_G$  close to 90% and around 20-30% would be expected in water and in lubricant, respectively. Removal efficiencies in PDMS 20 and in transformer oil would be included between those in water and in lubricant at a given value of  $A$ . These two solvents have similar viscosities. Nonetheless, PDMS 20 has a molar volume more than ten times higher than transformer oil, increasing  $D_L$  and  $k_L$ , which leads finally to slightly higher values of  $E_G$ . Nonetheless, for economic reasons, transformer oil should be preferred considering its waste status.

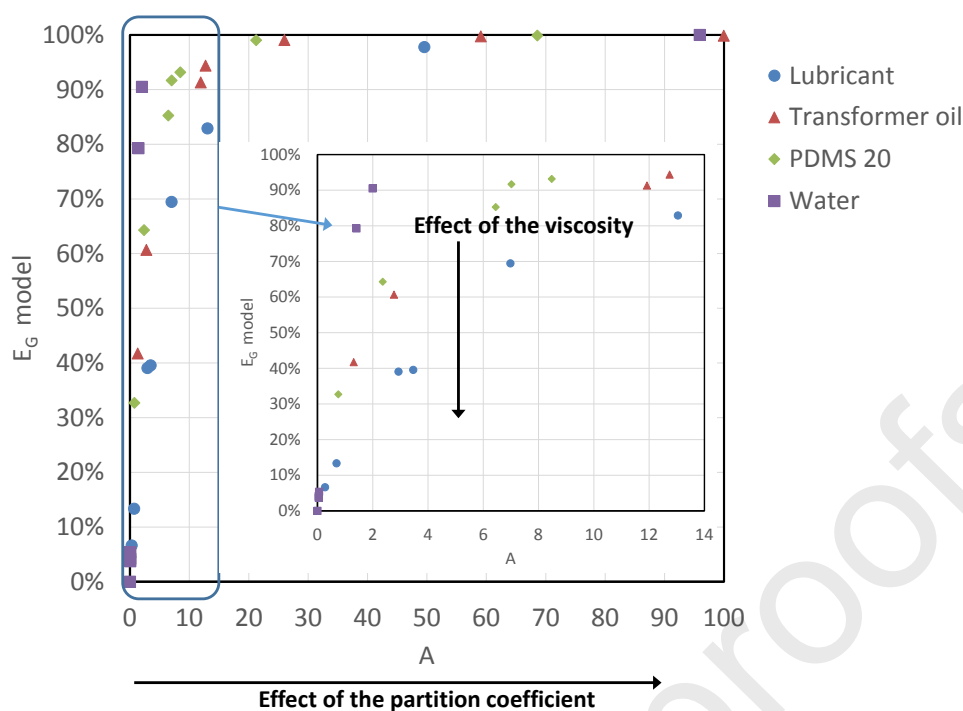


Figure 4: Modeled removal efficiency (adjusted SSR model) against the absorption factor  $A$  for the four solvents.

#### 4. Conclusions

The aim of this study was to investigate the absorption of seven non-polar and polar VOCs in two viscous waste oils, silicone oil and water in a laboratory-scale structured packing (internal diameter of 0.12 m). Removal efficiencies and overall volumetric mass transfer coefficients  $K_L a^\circ$  were measured for  $L/G$  ratios ranging from 1.5 to 10.2 depending on the solvent, and the overall volumetric mass transfer coefficients  $K_L a^\circ$  were deduced from the removal efficiencies using the NTU-HTU method.

Measured removal efficiencies confirmed the potential of transformer oil for the absorption of hydrophobic VOCs, with removal efficiencies higher than 80-90 % using only a 1 m height packed column. On the contrary, owing to a higher viscosity, not compensated by better affinities for VOC, the measured removal efficiencies in lubricant were significantly lower.

The Higbie penetration theory was applied to deconvolute  $K_L a^\circ$ , allowing to determine the local liquid and gas-side mass transfer coefficients  $k_L$  and  $k_G$ . These coefficients were compared to those calculated with the BS and SSR models. The SSR model describes accurately the influence of the solvent viscosity on  $K_L a^\circ$ . Nonetheless, this model overestimates  $K_L a^\circ$  with an average relative error of 83%. Thus, a corrective factor was applied to  $K_L a^\circ$ ,

allowing to decrease its relative error to 32%. With this modified model, the removal efficiency was predicted by the NTU-HTU method with a relative error of 7% and no bias related to the solvent viscosity (14% with the original model but in that case the removal efficiency is always overestimated by the model). Consequently, with the SSR model, the removal efficiency can be fairly predicted in a given packed column knowing only the partition coefficient and the solvent properties (viscosity, density, molar mass and surface tension) avoiding time-consuming and expensive lab-scale or semi-industrial scale experiments.

This study demonstrates that absorption of hydrophobic VOCs in viscous waste oils could be a feasible technical option. Nonetheless, high volumes of waste oils would be necessary for an industrial application. In that case, a solvent regeneration unit might be necessary making a technical and economical feasibility study necessary.

## 5. Acknowledgments

We are very grateful to the French Association Nationale de la Recherche et de la Technologie (ANRT) for the CIFRE PhD grant N° 2016/0238 attributed to Margaux Lhuissier, and also to the French governmental agency ADEME for the CORTEA funding n°1881C0001. We would like to thank our industrial partner Chimirec for providing the waste oils used in this study and their partnership in this study.

## 6. Nomenclature

$A$ : absorption factor (defined Eq. 2)

$A_p$ : specific surface area of packing ( $\text{m}^2 \text{m}^{-3}$ )

$a^\circ$ : interfacial area relative to the packing volume ( $\text{m}^2 \text{m}^{-3}$ )

$ARE$ : Average Relative Error

$BS$ : Billet-Schultes

$C_{G,in}$  and  $C_{G,out}$ : inlet concentration and outlet concentration in the gas phase ( $\text{mg m}^{-3}$  or ppmv)

$C_v, C_L$ : constants relative to each commercial packing according to Billet-Schultes

$d_h$ : hydraulic diameter =  $4\varepsilon/a$  (m)

DEHA: di-2-ethylhexyladipate

$D_L, D_G$ : diffusion coefficient in the liquid and in the gas phase ( $\text{m}^2 \text{s}^{-1}$ )

$D_{col}$ : column diameter (m)

$E_G$ : removal efficiency

$F$ : volume flowrate ( $\text{m}^3 \text{h}^{-1}$  or  $\text{m}^3 \text{s}^{-1}$ )

$g$ : specific gravity constant ( $9.81 \text{ m s}^{-2}$ )

$G$ : gas mass flowrate ( $\text{kg s}^{-1}$ )

$h_L$ : liquid holdup (-)

$HTU_{OL}$ : overall height of a transfer unit in the liquid phase (m)  $= \frac{F_L}{S_{col} \times K_L a^\circ}$

$k_G$ : local gas-side mass transfer coefficient ( $\text{m s}^{-1}$ )

$k_L$ : local liquid-side mass transfer coefficient ( $\text{m s}^{-1}$ )

$K_L$ : overall liquid-side mass transfer coefficient ( $\text{m s}^{-1}$ )

$K_L a^\circ$ : overall volumetric mass transfer coefficient in the liquid phase ( $\text{s}^{-1}$ )

$L$ : liquid mass flowrate ( $\text{kg s}^{-1}$ )

MIBK: methylisobutylketone

NAPL: non-aqueous phase liquid

$NTU_{OL}$ : overall number of transfer units in the liquid phase  $= \frac{1}{A-1} \ln \left( \frac{A-E_G}{A(1-E_G)} \right)$

PDMS: polydimethylsiloxane

$U$ : superficial velocity ( $\text{m s}^{-1}$ )

VOC: volatile organic compound

$Z$ : packing height (m)

$R$ : ideal gas constant (8.314 J mol<sup>-1</sup> K<sup>-1</sup>)

$RE$ : Relative error (in absolute value)

$R_L$ : relative resistance of the liquid phase (dimensionless)

$T$ : temperature (K)

TMB: trimethylbenzene

$S_{col}$ : column section (m<sup>2</sup>)

SSR: Song-Seibert-Rochelle

$V_{mol}$ : molar volume (cm<sup>3</sup> mol<sup>-1</sup>)

#### Greek letters

$\varepsilon$ : packing void fraction (-)

$\rho$ : density (kg.m<sup>-3</sup>)

$\mu$ : dynamic viscosity (Pa s)

$\tau$ : renewal times of fluid elements at the gas-liquid interface (s)

#### Subscripts

G: relative to the gas phase

L: Relative to the liquid phase

O: overall

## 7. REFERENCES

- Bay, K., Wanko, H., Ulrich, J., 2006. Absorption of volatile organic compounds in biodiesel: determination of infinite dilution activity coefficients by headspace gas chromatography. *Chemical Engineering Research and Design* 84, 22–28.
- Biard, P.-F., Coudon, A., Couvert, A., Giraudet, S., 2016. A simple and timesaving method for the mass-transfer assessment of solvents used in physical absorption. *Chemical Engineering Journal* 290, 302–311. <https://doi.org/10.1016/j.cej.2016.01.046>
- Biard, P.-F., Couvert, A., 2013. Overview of mass transfer enhancement factor determination for acidic and basic compounds absorption in water. *Chem. Eng. J.* 222, 444–453.
- Biard, P.-F., Couvert, A., Giraudet, S., 2018. Volatile organic compounds absorption in packed column: theoretical assessment of water, DEHA and PDMS 50 as absorbents. *J. Indus. Eng. Chem.* 59, 70–78.
- Biard, P.-F., Couvert, A., Renner, C., 2017. Intensification of volatile organic compound absorption in a compact wet scrubber at co-current flow. *Chemosphere* 173, 612–621.
- Billet, R., Schultes, M., 1999. Prediction of mass transfer columns with dumped and arranged packings: updated summary of the calculation method of Billet and Schultes. *Chem. Eng. Res. Des.* 77, 498–504.
- Billet, R., Schultes, M., 1993a. A physical model for the prediction of liquid hold-up in two-phase countercurrent columns. *Chem. Eng. Technol.* 16, 370–375.
- Billet, R., Schultes, M., 1993b. Predicting mass transfer in packed columns. *Chem. Eng. Technol.* 16, 1–9.
- Billet, R., Schultes, M., 1991. Modelling of pressure drop in packed columns. *Chem. Eng. Technol.* 14, 89–95.
- Bourgeois, D., Thomas, D., Fanlo, J.L., Vanderschuren, J., 2006. Solubilities at high dilution of toluene, ethylbenzene, 1, 2, 4-trimethylbenzene, and hexane in di-2-ethylhexyl, diisooheptyl, and diisononyl phthalates. *Journal of Chemical Engineering Data* 51, 1212–1215.
- Bourgeois, D., Vanderschuren, J., Thomas, D., 2008. Determination of liquid diffusivities of VOC (paraffins and aromatic hydrocarbons) in phthalates. *Chemical Engineering & Processing: Process Intensification* 47, 1363–1370.
- Brunazzi, E., Paglianti, A., Spiegel, L., Tolaini, F., 2002. Hydrodynamics of a gas-liquid column equipped with MellapakPlus packing, in: *International Conference on Distillation and Absorption*.
- Bruneel, J., Walgraeve, C., Dumortier, S., Stockman, J., Demeyer, P., Van Langenhove, H., 2018. Increasing mass transfer of volatile organic compounds in air scrubbers: a fundamental study for different gas-liquid systems. *Journal of Chemical Technology & Biotechnology* 93, 1468–1476.
- Busca, G., Pistarino Chiara, 2003a. Technologies for the abatement of sulphide compounds from gaseous streams: a comparative overview. *Journal of Loss Prevention in the Process Industries* 16, 363–371.
- Busca, G., Pistarino Chiara, 2003b. Abatement of ammonia and amines from waste gases : a summary. *Journal of Loss Prevention in the Process Industries* 16, 157–163.
- Camper, D., Becker, C., Koval, C., Noble, R., 2006. Diffusion and Solubility Measurements in Room Temperature Ionic Liquids. *Ind. Eng. Chem. Res.* 45, 445–450. <https://doi.org/10.1021/ie0506668>
- Chiang, C.-Y., Liu, Y.-Y., Chen, Y.-S., Liu, H.-S., 2012. Absorption of Hydrophobic Volatile Organic Compounds by a Rotating Packed Bed. *Ind. Eng. Chem. Res.* 51, 9441–9445. <https://doi.org/10.1021/ie2021637>
- Darracq, G., Couvert, A., Couriol, C., Amrane, A., Le Cloirec, P., 2012. Removal of Hydrophobic Volatile Organic Compounds in an Integrated Process Coupling Absorption and Biodegradation—Selection of an Organic Liquid Phase. *Water, Air, & Soil Pollution* 223, 4969–4997.
- Darracq, G., Couvert, A., Couriol, C., Amrane, A., Le Cloirec, P., 2010a. Integrated process for hydrophobic VOC treatment—solvent choice. *Can. J. Chem. Eng.* 88, 655–660.
- Darracq, G., Couvert, A., Couriol, C., Amrane, A., Thomas, D., Dumont, E., Andres, Y., Le Cloirec, P., 2010b. Silicone oil: An effective absorbent for the removal of hydrophobic volatile organic compounds. *Journal of Chemical Technology & Biotechnology* 85, 309–313. <https://doi.org/10.1002/jctb.2331>
- Dumont, É., 2018. Mass transfer in multiphasic gas/liquid/liquid systems. KLa determination using the effectiveness-number of transfer unit method. *Processes* 6, 156.
- Dumont, E., Darracq, G., Couvert, A., Couriol, C., Amrane, A., Thomas, D., Andrés, Y., Le Cloirec, P., 2012. Hydrophobic VOC absorption in two-phase partitioning bioreactors; influence of silicone oil volume fraction on absorber diameter. *Chemical Engineering Science* 71, 146–152. <https://doi.org/10.1016/j.ces.2011.12.017>
- Ferguson, L., Scovazzo, P., 2007. Solubility, Diffusivity, and Permeability of Gases in Phosphonium-Based Room Temperature Ionic Liquids: Data and Correlations. *Ind. Eng. Chem. Res.* 46, 1369–1374. <https://doi.org/10.1021/ie0610905>

- Guihéneuf, S., Castillo, A.S.R., Paquin, L., Biard, P.-F., Couvert, A., Amrane, A., 2014. Absorption of Hydrophobic Volatile Organic Compounds in Ionic Liquids and Their Biodegradation in Multiphase Systems, in: *Production of Biofuels and Chemicals with Ionic Liquids*. Springer, pp. 305–337.
- Guillerm, M., Couvert, A., Amrane, A., Dumont, É., Norrant, E., Lesage, N., Juery, C., 2015. Characterization and selection of PDMS solvents for the absorption and biodegradation of hydrophobic VOCs. *J. Chem. Technol. Biotechnol.* 95, 1923–1927.
- Guillerm, M., Couvert, A., Amrane, A., Norrant, E., Lesage, N., Dumont, E., 2016. Absorption of toluene in silicone oil: Effect of the solvent viscosity on hydrodynamics and mass transfer. *Chemical Engineering Research and Design* 109, 32–40.
- Hadjoudj, R., Monnier, H., Roizard, C., Lapicque, F., 2008. Measurements of diffusivity of chlorinated VOCs in heavy absorption solvents using a laminar falling film contactor. *Chemical Engineering and Processing: Process Intensification* 47, 1478–1483.
- Hadjoudj, R., Monnier, H., Roizard, C., Lapicque, F., 2004. Absorption of Chlorinated VOCs in High-Boiling Solvents: Determination of Henry's Law Constants and Infinite Dilution Activity Coefficients. *Ind. Eng. Chem. Res.* 43, 2238–2246. <https://doi.org/10.1021/ie0304006>
- Hayduk, W., Laudie, H., 1974. Prediction of diffusion coefficients for nonelectrolytes in dilute aqueous solutions. *AIChE Journal* 20, 611–615. <https://doi.org/10.1002/aic.690200329>
- Heymes, Frederic, Demoustier, P.M., Charbit, F., Fanlo, J.L., Moulin, P., 2006. Hydrodynamics and mass transfer in a packed column: case of toluene absorption with a viscous absorbent. *Chem. Eng. Sci.* 61, 5094–5106.
- Heymes, Frédéric, Manno-Demoustier, P., Charbit, F., Fanlo, J.L., Moulin, P., 2006. A new efficient absorption liquid to treat exhaust air loaded with toluene. *Chem. Eng. J.* 115, 225–231.
- Higbie, R., 1935. The rate of absorption of a pure gas into still liquid during short periods of exposure. *Transactions of American Institute of Chemical Engineers* 35, 365–389.
- Khan, F.I., Ghoshal, A.K., 2000. Removal of Volatile Organic Compounds from polluted air. *Journal of Loss Prevention in the Process Industries* 13, 527–545.
- Lalanne, F., Malhautier, L., Roux, J.-C., Fanlo, J.-L., 2008. Absorption of a mixture of volatile organic compounds (VOCs) in aqueous solutions of soluble cutting oil. *Bioresource technology* 99, 1699–1707.
- Lhuissier, M., Couvert, A., Amrane, A., Kane, A., Audic, J.-L., 2018. Characterization and selection of waste oils for the absorption and biodegradation of VOC of different hydrophobicities. *Chemical Engineering Research and Design* 138, 482–489. <https://doi.org/10.1016/j.cherd.2018.08.028>
- Lhuissier, M., Couvert, A., Kane, A., Amrane, A., Audic, J.-L., Biard, P.-F., 2020. Experimental evaluation and modeling of the hydrodynamics in structured packing operated with viscous waste oils. *Chemical Engineering Research and Design* 162, 273–283.
- Mhiri, N., Monnier, H., Falk, L., 2011. Intensification of the G/L absorption in microstructured falling film application to the treatment of chlorinated VOC's. Part III: Influence of gas thickness channel on mass transfer. *Chemical Engineering Science* 66, 5989–6001. <https://doi.org/10.1016/j.ces.2011.08.021>
- Minne, U.L., Burger, A.J., Schwarz, C.E., 2018. The effect of fluid properties and packing size on the hydrodynamics of packed columns. *Chemical Engineering Transactions* 69, 31–36.
- Monnier, H., Falk, L., 2011. Intensification of G/L absorption in microstructured falling film. Application to the treatment of chlorinated VOC's - part II: Modeling and geometric optimization. *Chemical Engineering Science* 66, 2475–2490. <https://doi.org/10.1016/j.ces.2011.01.016>
- Monnier, H., Falk, L., Lapicque, F., Hadjoudj, R., Roizard, C., 2010. Intensification of G/L absorption in microstructured falling film. Application to the treatment of chlorinated VOC's – part I: Comparison between structured and microstructured packings in absorption devices. *Chemical Engineering Science* 65, 6425–6434. <https://doi.org/10.1016/j.ces.2010.09.027>
- Morgan, D., Ferguson, L., Scovazzo, P., 2005. Diffusivities of Gases in Room-Temperature Ionic Liquids: Data and Correlations Obtained Using a Lag-Time Technique. *Ind. Eng. Chem. Res.* 44, 4815–4823. <https://doi.org/10.1021/ie048825v>
- Muñoz, R., Daugulis, A.J., Hernández, M., Quijano, G., 2012. Recent advances in two-phase partitioning bioreactors for the treatment of volatile organic compounds. *Biotechnology Advances* 30, 1707–1720. <https://doi.org/10.1016/j.biotechadv.2012.08.009>
- Muñoz, R., Villaverde, S., Guieysse, B., Revah, S., 2007. Two-phase partitioning bioreactors for treatment of volatile organic compounds. *Biotechnology Advances* 25, 410–422. <https://doi.org/10.1016/j.biotechadv.2007.03.005>
- Ozturk, B., Yilmaz, D., 2006. Absorptive Removal of Volatile Organic Compounds from Flue Gas Streams. *Process Safety and Environmental Protection* 84, 391–398. <http://dx.doi.org/10.1205/psep05003>

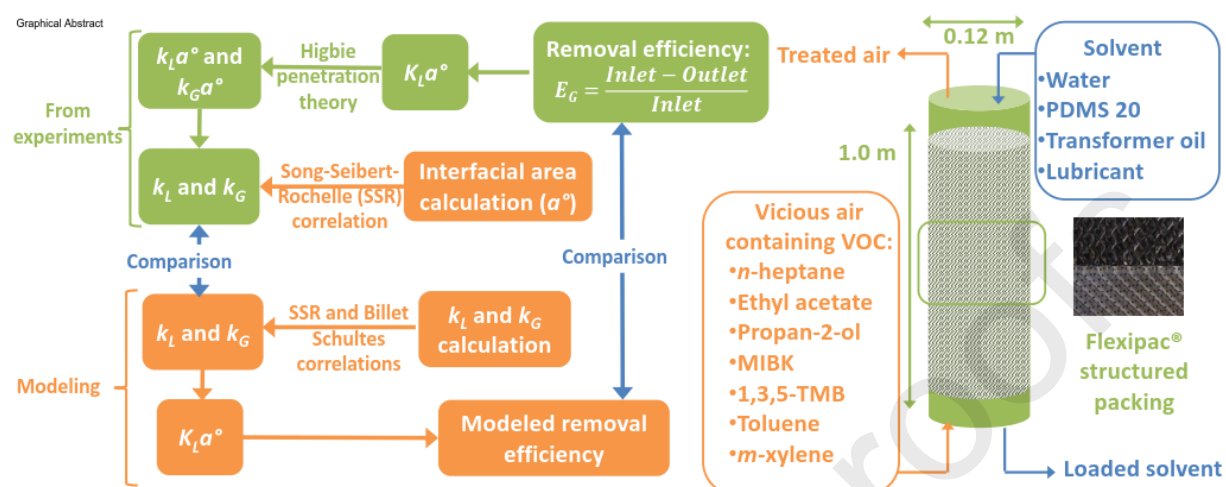
- Patel, M.J., Papat, S.C., Deshusses, M.A., 2016. Determination and Correlation of the Partition Coefficients of 48 Volatile Organic and Environmentally Relevant Compounds Between Air and Silicone Oil. *Chem. Eng. J.* 310, 72–78. <http://dx.doi.org/10.1016/j.cej.2016.10.086>
- Perry, R.H., Green, D.W., 1997. *Perry's chemical engineers' handbook*, 7th edition. McGraw-Hill, New-York.
- Quijano, G., Couvert, A., Amrane, A., Darracq, G., Couriol, C., Le Cloirec, P., Paquin, L., Carrié, D., 2011. Potential of ionic liquids for VOC absorption and biodegradation in multiphase systems. *Chem. Eng. Sci.* 66, 2707–2712. <https://doi.org/10.1016/j.ces.2011.01.047>
- Rodriguez Castillo, A.S., Biard, P.-F., Guihéneuf, S., Paquin, L., Amrane, A., Couvert, A., 2019. Assessment of VOC absorption in hydrophobic ionic liquids: Measurement of partition and diffusion coefficients and simulation of a packed column. *Chem. Eng. J.* 360, 1416–1426. <https://doi.org/10.1016/j.cej.2018.10.146>
- Roustan, M., 2003. *Transferts gaz-liquide dans les procédés de traitement des eaux et des effluents gazeux*. Lavoisier, Paris.
- Ruddy, E.N., Carroll, L.A., 1993. Select the best VOC control strategy. *Chemical engineering progress* 89, 28–35.
- Sangster, J., 1989. Octanol-water partition coefficients of simple organic compounds. *Journal of Physical and Chemical Reference Data* 18, 1111–1229.
- Shiflett, M.B., Harmer, M.A., Junk, C.P., Yokozeki, A., 2006. Solubility and diffusivity of 1,1,1,2-tetrafluoroethane in room-temperature ionic liquids. *Fluid Phase Equilibria* 242, 220–232. <http://dx.doi.org/10.1016/j.fluid.2006.01.026>
- Shiflett, M.B., Yokozeki, A., 2006. Solubility and diffusivity of hydrofluorocarbons in room-temperature ionic liquids. *AIChE J.* 52, 1205–1219. <https://doi.org/10.1002/aic.10685>
- Song, D., Seibert, A.F., Rochelle, G.T., 2018. Mass Transfer Parameters for Packings: Effect of Viscosity. *Industrial & Engineering Chemistry Research* 57, 718–729. <https://doi.org/10.1021/acs.iecr.7b04396>
- Song, D., Seibert, A.F., Rochelle, G.T., 2014. Effect of Liquid Viscosity on the Liquid Phase Mass Transfer Coefficient of Packing. *Energy Procedia* 63, 1268–1286. <https://doi.org/10.1016/j.egypro.2014.11.136>
- Staudinger, J., Roberts, P.V., 2001. A critical compilation of Henry's law constant temperature dependence relations for organic compounds in dilute aqueous solutions. *Chemosphere* 44, 561–576.
- Tatin, R., Moura, L., Dietrich, N., Baig, S., Hébrard, G., 2015. Physical absorption of volatile organic compounds by spraying emulsion in a spray tower: Experiments and modelling. *Chemical Engineering Research and Design* 104, 409–415. <https://doi.org/10.1016/j.cherd.2015.08.030>
- Vuong, M.D., Couvert, A., Couriol, C., Amrane, A., Le Cloirec, P., Renner, C., 2009. Determination of the Henry's constant and the mass transfer rate of VOCs in solvents. *Chem. Eng. J.* 150, 426–430. <http://dx.doi.org/10.1016/j.cej.2009.01.027>

## 8. Appendix

Table A.1: Octanol-water partition coefficient (Log P) (Sangster, 1989), Diffusivities in the gas phase and in the liquid phase at 25°C of the seven VOCs in the four solvents. For the diffusivities in the liquid phase in the three NAPLs, two correlations, those of Wilke-Chang (#1) and those of Rodriguez *et al.* (#2) were considered (Rodriguez Castillo *et al.*, 2019; Roustan, 2003). In water, the correlation of Hayduk and Laudie was used (Hayduk and Laudie, 1974; Roustan, 2003). The diffusivity in air was calculated using the Fuller *et al.* correlation (Perry and Green, 1997; Roustan, 2003).

|               | Log P | $10^6 \times D_G$<br>$m^2 s^{-1}$ | $V_{mol}$<br>$cm^3 mol^{-1}$ | $10^{11} \times D_L$ in lubricant<br>$m^2 s^{-1}$ |      | $10^{11} \times D_L$ in transformer oil<br>$m^2 s^{-1}$ |      | $10^{10} \times D_L$ in PDMS 20<br>$m^2 s^{-1}$ |      | $10^{10} \times D_L$ in water<br>$m^2 s^{-1}$ |
|---------------|-------|-----------------------------------|------------------------------|---|------|---|------|---|------|---|
|               |       |                                   |                              | #1  | #2   | #1  | #2   | #1  | #2   |   |
|               |       |                                   |                              | n-heptane   | 4.50 | 7.05  | 163  | 3.98  | 2.54 |   |
| Ethyl acetate | 0.73  | 8.70                              | 106.3                        | 5.14  | 5.09 | 16.3  | 11.5 | 3.67  | 3.04 | 9.50  |
| Isopropanol   | 0.25  | 10.2                              | 82.2                         | 6.00  | 7.73 | 19.0  | 17.5 | 4.29  | 4.62 | 11.1  |
| MIBK          | 1.31  | 7.49                              | 134.0                        | 4.48  | 3.50 | 14.2  | 7.90 | 3.20  | 2.09 | 8.27  |
| Toluene       | 2.73  | 7.54                              | 118.5                        | 4.82  | 4.27 | 15.3  | 9.64 | 3.44  | 2.55 | 8.90  |
| m-xylene      | 3.20  | 6.96                              | 106.2                        | 4.35  | 3.24 | 13.8  | 7.33 | 3.11  | 1.94 | 8.04  |
| TMB           | 3.42  | 6.50                              | 120.2                        | 4.08  | 2.73 | 12.9  | 6.16 | 2.92  | 1.63 | 7.54  |

## Graphical abstract



### Highlights

- Absorption efficiencies of 7 VOCs were measured in a 1 m height structured packing
- Lubricant and transformer waste oils were investigated
- Removal efficiencies up to 80-90% were measured for hydrophobic VOCs in transformer oil
- Overall mass transfer coefficients were deconvoluted to determine local coefficients
- The Song-Seibert-Rochelle models fairly predicted the influence of the viscosity on mass-transfer

Credit author statement

Margaux Lhuissier: Conceptualization, validation, formal analysis, investigation, Writing – Original Draft, visualization

Annabelle Couvert : Conceptualization, Investigation, Resources, Supervision, Writing- Review and Editing, Project administration, Funding acquisition

Abdoulaye Kane : Conceptualization, Resources, Writing- Review and Editing

Abdeltif Amrane : Conceptualization, Methodology, Writing- Review and Editing

Jean-Luc Audic : Investigation, Resources, Supervision, Project administration, writing – original draft

Pierre-François Biard : conceptualization, methodology, formal analysis, data curation, writing – original draft, Writing - Review & Editing, vizualisation